group appears to vary from molecule to molecule. In the solid methyl pheophorbide *a*, the vinyl C_β atom is ca. 0.23 Å out of the macrocyclic ring plane pointing toward the C_1 Me, whereas in ethyl chlorophyllide it is ca. 0.5 Å out of the plane pointing toward the C_α methine. Also, Katz[30] has noted the varying β-proton shift sequences in the vinyl group in chlorin e_6 and protoporphyrin IX and interpreted them as due to different orientations of the vinyl groups in the two molecules. Clearly, the orientation of the vinyl group is delicately balanced in these molecules, and thus it is not surprising that ketal formation (in **3** and **4**) could be sufficient to change the orientation in the chlorin with respect to the porphyrin.

Experimental Section

Proton NMR spectra were obtained in $CDCl_3$ solution on a Nicolet NT-360 pulsed FT spectrometer, using 16K data points with a 3-kHz sweep width. The internal reference was the residual $CHCl_3$ line, assigned to 7.26 ppm.

Melting points were measured on a microscopic hot-stage apparatus and are uncorrected. TLC monitoring of reactions was performed with Merck silica gel 60 F254 precoated sheets (0.2 mm), and column chromatography was carried out with Merck neutral alumina (70–230 mesh). Electronic absorption spectra were measured with solutions in methylene chloride on a HP 8450A spectrophotometer.

Methyl pheophorbide *a* was obtained by large-scale extraction of the blue-green alga *Spirulina maxima*.[31] Zinc was inserted into the chlorophyll derivatives by standard methodology.[32]

9-Ketal (3) of Methyl Pyropheophorbide *a*. Methyl pheophorbide *a* (2 g) was heated under reflux in collidine[16] (150 mL) for 90 min during slow passage of a stream of N_2 throught the mixture. The solution was evaporated to dryness under vacuum, and the residue was taken up in toluene (200 mL) and dry dioxane (10 mL) containing ethylene glycol (4 mL) and *p*-toluenesulfonic acid (100 mg). This mixture was heated under reflux with a Dean-Stark trap for 3 days, after which time analytical TLC showed a fast-moving spot. After being passed through a bed of alumina (Brockman Grade III), the solution was washed with saturated aqueous $NaHCO_3$ and water and then dried over anhydrous Na_2SO_4. The solution was then evaporated to dryness under vacuum and the residue was chromatographed on alumina (Brockmann Grade III; elution with methylene chloride). The ketal formed a fast-moving green band, and this was followed by a second band, which afforded methyl pyropheophorbide *a* (700 mg), identical with an authentic sample. The eluates containing the ketal were evaporated to dryness, and the product **3** was crystallized from CH_2Cl_2/*n*-hexane to give 1.131 g (59%): mp 182-184 °C; λ_{max} 300 nm (ϵ 12 000), 391 (93 000), 500 (13 800), 598 (3 800), 654 (41 000). Anal. Calcd for $C_{36}H_{40}N_4O_4$: C, 72.94; H, 6.80; N, 9.45. Found: C, 72.98; H, 6.82; N, 9.33.

9-Ketal (4) of 2-Vinylphylloerythrin Methyl Ester. The chlorin ketal **3** (300 mg) in methylene chloride (200 mL) was stirred at 0 °C (ice bath) and treated with 77.5 mL of a DDQ solution (435 mg of DDQ in 250 mL of benzene), dropwise. The resulting mixture was monitored by analytical TLC, the reaction being deemed complete when the green ketal chlorin had been compleely transformed into a red ketal porphyrin spot. The mixture was then filtered through a short bed of alumina (Brockmann Grade III), and the red solution was evaporated to dryness. Crystallization of the residue from CH_2Cl_2/benzene gave 241 mg (81%) of the ketal porphyrin: mp >300 °C; λ_{max} 412 nm (ϵ 92 900), 508 (15 200), 546 (10 300), 570 (8900), 622(1400). Anal. Calcd. for $C_{36}H_{38}H_4O_4$: C, 73.20; H, 6.48; N, 9.48. Found: C, 72.92; H, 6.48; N, 9.29.

2-Vinylphylloerythrin Methyl Ester (2). The foregoing ketal porphyrin **4** (200 mg) in tetrahydrofuran (1 L) and acetone (300 mL) was shaken for 10 min with 0.3 M aqueous HCl (300 mL) and then poured into methylene chloride (500 mL) and washed 3 times with water (1 L). The organic phase was dried (Na_2SO_4) and evaporated to dryness, and the residue was crystallized from CH_2Cl_2/MeOH to give 2-vinylphylloerythrin methyl ester (181 mg; 98%), mp 277-280 °C (lit.[15] mp 278 °C).

Acknowledgment. This research was supported by grants from the National Science Foundation and the Scientific Affairs Division of NATO (RG 256.80).

(30) Reference 14, p 504.
(31) Wasielewski, M. R.; Smith, R. L.; Kostka, A. G. *J. Am. Chem. Soc.* **1980**, *102*, 6923–6928.
(32) Fuhrhop, J.-H.; Smith, K. M. "Laboratory Methods in Porphyrin and Metalloporphyrin Research"; Elsevier: Amsterdam, 1975; p 42.

Vinyl Influences on Protoheme Resonance Raman Spectra: Nickel(II) Protoporphyrin IX with Deuterated Vinyl Groups

S. Choi,[†] T. G. Spiro,*[,†] K. C. Langry,[‡] and K. M. Smith[‡]

Contribution from the Departments of Chemistry, Princeton University, Princeton, New Jersey 08544, and the University of California, Davis, California 95616.
Received June 19, 1981

Abstract: Infrared absorption and variable excitation (4067, 4131, 5145, and 5682 Å, near the B, Q_1, and Q_0 absorption maxima) resonance Raman spectra are reported for NiPP (PP = protoporphyrin IX dimethyl ester) and for NiPP-d_α (vinyl α-carbons deuterated) and NiPP-$d_{2\beta}$ (vinyl β-carbons dideuterated). The deuteration shifts and comparison with NiOEP (OEP = octaethylporphyrin) permit identification of most of the vinyl modes and correlation of the protoporphyrin skeletal modes with those of OEP. Strong interactions with skeletal modes are evident in splittings of some of the vinyl modes and are probably responsible for the vinyl mode Raman enhancements. They also shift some of the skeletal mode frequencies, relative to NiOEP, but several skeletal modes are unshifted, including some previously identified as heme structure markers. The vinyl groups induce Raman activity into several infrared modes, reflecting the asymmetric conjugation in PP. No IR activity is seen for Raman modes, however, suggesting that vinyl conjugation occurs primarily in the excited state.

Resonance Raman (RR) spectroscopy is increasingly seen as a powerful tool for the study of heme protein structure and dynamics.[1-9] If it is to reach its full potential, the spectra must be properly assigned, and the nature of the vibrations being monitored must be understood. Much progress has been made in this direction through the study, in many laboratories, of metalloporphyrin RR systematics. An important step was taken by Kitagawa and co-workers,[10] who assigned all of the in-plane skeletal Raman modes of NiOEP (OEP = octaethylporphyrin),

[†] Princeton University.
[‡] University of California, Davis.

(1) Spiro, T. G. *Isr. J. Chem.* **1981**, *21*, 81.
(2) Nagai, K.; Kitagawa, T. *Proc. Natl. Acad. Sci. U.S.A.* **1980**, *77*, 2033.
(3) Rousseau, D. L.; Shelnutt, J. A.; Henry, E. R.; Simon, S. R. *Nature (London)* **1980**, *285*, 49.
(4) Friedman, J. M.; Lyons, K. B. *Nature, (London)* **1980** *284*, 570.
(5) Shelnutt, J. A.; Rousseau, D. L.; Friedman, J. M.; Simon, A. R. *Proc. Natl. Acad. Sci. U.S.A.* **1979**, *76*, 4409.
(6) Yu, Nai-Teng; Srivastava, R. B. *J. Raman Spectrosc.* **1980**, *9*, 166.

0002-7863/82/1504-4337$01.25/0

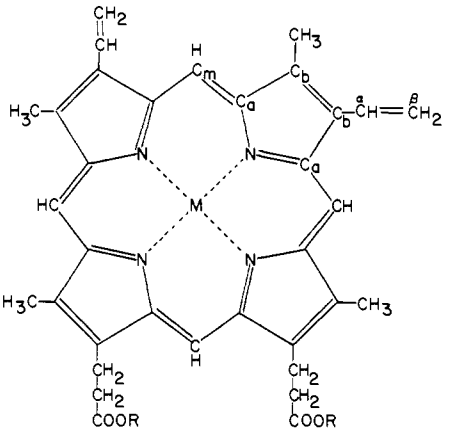

Figure 1. Structure of protoporphyrin IX, with atom labeling. In octaethylporphyrin, all the C_b substituents are replaced by ethyl groups.

using variable-wavelength excitation, polarization measurements, and analysis of combination modes; they also identified most of the infrared skeletal modes. A normal coordinate analysis[11] gave a reasonable fit to the observed frequencies and provided an assessment of the normal mode composition.

It was early recognized[12,13] that the peripheral vinyl groups of protoporphyrin IX, the most common porphyrin variant in heme proteins, could contribute to the RR spectra and that such contributions could explain the added RR complexity of protoheme proteins such as hemoglobin[12] and cytochrome b_5,[13] relative to cytochrome *c*, in which the vinyl groups are saturated via condensation with cysteine side chains. Understanding the vinyl contributions is important, not only for dealing with this complexity but also because they may provide a means of monitoring the interactions of the vinyl groups with protein residues. The role of such interactions in controlling O_2 binding and cooperativity[14-16] is of much current interest.

In the present work, we disentangle the vinyl contributions to the NiPP (PP = protoporphyrin IX dimethyl ester) vibrational spectrum by examining Raman and infrared shifts induced by deuteration of the vinyl C_α or C_β carbon atoms. The nickel complex was chosen because of the nearly complete assignments available for NiOEP,[10] which serves as a reference for the perturbing effects of the vinyl groups. RR spectra have also been recorded for iron complexes of PP, in various ligation and oxidation states, and for myoglobin derivatives. These serve as a basis for new RR spectra–structure correlations and for the analysis of protein influences, as described in the following paper.[17] In the course of this work we have observed RR bands for certain iron complexes that appear to arise from porphyrin out-of-plane deformations and that may prove useful as sensitive monitors of porphyrin conformation.[18]

Results

Figure 1 shows the protoporphyrin IX structure and atom labeling. Raman spectra were recorded for its Ni[II] complex (as the dimethyl ester in CCl_4 or CH_2Cl_2 solution) and for the deuterated forms, NiPP-d_α (the α-carbon atoms of *both* vinyl groups deuterated) and NiPP-$d_{2\beta}$ (the pair of H atoms on the β-carbon atom of both vinyl groups replaced by D). These spectra are compared in Figures 2, 3, and 4 for laser excitation at 4131, 5145, and 5682 Å, close to resonance with B (403 nm), Q_1 (525 nm), and Q_0 (563 nm) absorption bands, respectively. Figure 5 shows the low-frequency RR spectra for these complexes, along with that of NiOEP, with 4067-Å excitation. Figure 6 compares their infrared (IR) spectra.

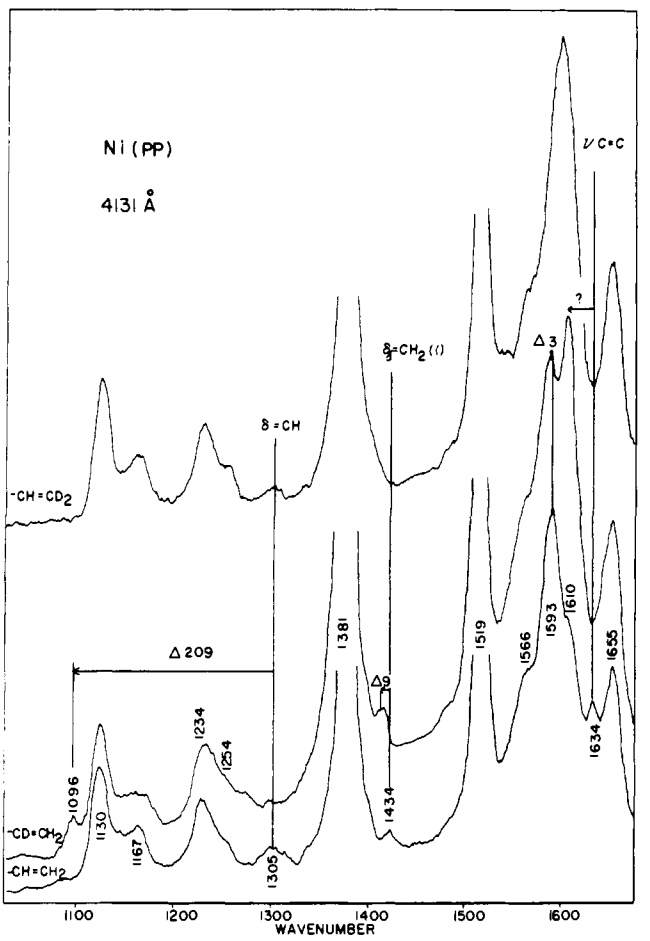

Figure 2. RR spectra of NiPP, NiPP-d_α, and NiPP-$d_{2\beta}$, in CCl_4 excited at 4131 Å. Conditions: laser power 100 mW, slit width 8 cm^{-1}, time constant 15 s, scanning speed 0.1 cm^{-1}/s.

Table I gives measured depolarization ratios for all the Raman bands of NiOEP and NiPP at the three excitation wavelengths. Table II lists all the RR and IR frequencies that can be assigned to prophyrin in-plane skeletal modes, including those involving the bonds between the C_b atoms and the peripheral substituents, and to modes of the vinyl groups. These assignments are discussed in the next section. The IR spectra contain a number of bands arising from local modes of the peripheral groups and from out-of-plane porphyrin skeletal deformations. These have not been analyzed. Figure 7 is a schematic diagram of the in-plane skeletal and vinyl assignments, intended as a guide to the ensuing discussion. The various modes are displayed in order of frequency, as solid (Raman) or dashed (IR) lines, capped with symbols identifying their approximate symmetry species. The sizes of the symbols indicate the relative intensities (strong, medium, or weak) of the RR bands, at the wavelength of greatest enhancement. For each skeletal mode, the major internal coordinate contributor is given, according to the calculation of Abe et al.[11] We have, however, reversed the major contributors, C_aC_m and C_bC_b, to the two highest E_u modes, ν_{37} and ν_{38}, on the basis of the meso deuteration shift of ν_{38}.[10]

Discussion

A. General Considerations. Metalloporphyrins have approximately D_{4h} symmetry and a characteristic three-banded (Q_0, Q_1, B) visible absorption spectrum, resulting from configuration interaction and vibronic mixing of the electronic transitions between

(7) Asher, S. A.; Schuster, T. M. *Biochemistry* **1979**, *18*, 5377.
(8) Woodruff, W. H.; Farguharson, S. *Science (Washington, D.C.)* **1978**, *201*, 831.
(9) Ondrias, M. R.; Findsen, E. W.; Leroi, G. E.; Babock, G.T. *Biochemistry* **1980**, *19*, 1723.
(10) Kitagawa, T.; Abe, M.; Ogoshi, H. *J. Chem. Phys.* **1979**, *69*, 4516.
(11) Abe, M.; Kitagawa, T.; Kyogoku, Y. *J. Chem. Phys.* **1978**, *69*, 4526.
(12) Spiro, T. G.; Strekas, T. C. *J. Am. Chem. Soc.* **1974**, *96*, 338.
(13) Adar, F. *Arch. Biochem. Biophys.* **1975**, *170*, 644. Adar, F.; Erecinska, M. *Ibid.* **1974**, *165*, 570.
(14) Asakura, T.; Sono, M. *J. Biol. Chem.* **1974**, *249*, 7087.
(15) Gellin, B.; Karplus, M. *Proc. Natl. Acad. Sci., U.S.A.* **1977**, *74*, 801.
(16) Warshel, A.; Weiss, R. M. *J. Am. Chem. Soc.* **1981**, *103*, 446.
(17) Choi, S.; Spiro, T. G.; Langry K. C.; Smith, K. M.; Budd, D. L.; La Mar G. N. *J. Am. Chem. Soc.*, following paper in this issue.
(18) Choi, S.; Spiro, T. G., to be published.

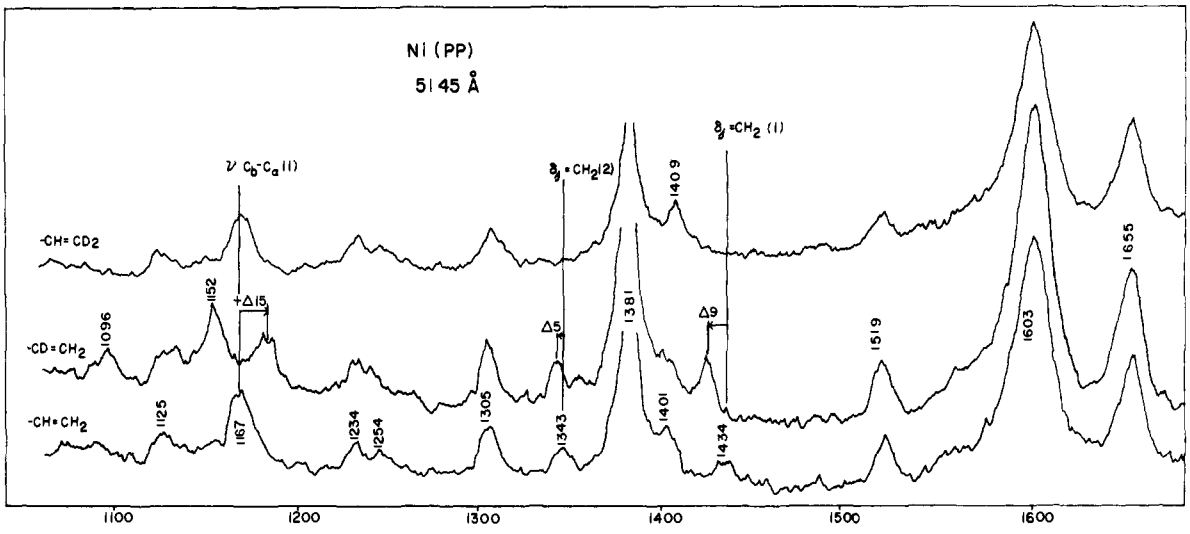

Figure 3. RR spectra of NiPP, NiPP-d_α, and NiPP-$d_{2\beta}$ in CCl_4 excited at 5145 Å. Conditions: laser power 250 mW, slit width 6 cm^{-1}, time constant 3 s, scanning speed 0.5 cm^{-1}/s.

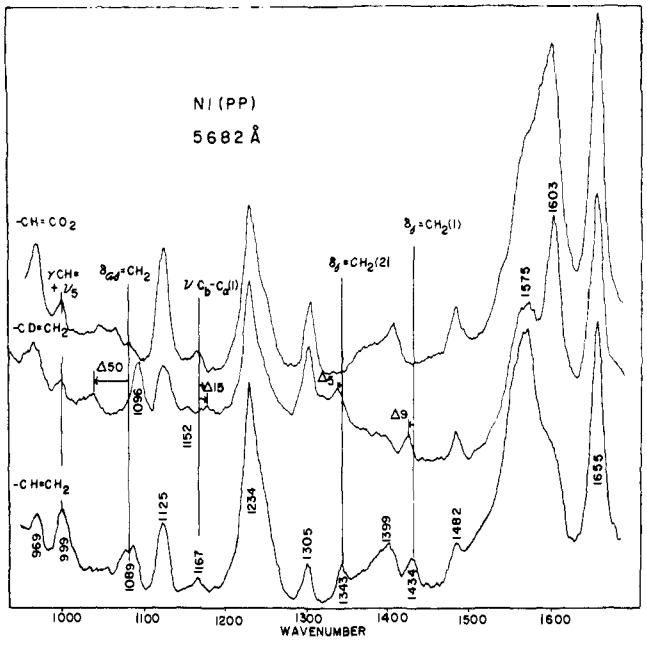

Figure 4. RR spectra of NiPP, NiPP-d_α and NiPP-$d_{2\beta}$ in CCl_4 excited at 5682 Å. Conditions: laser power 120 mW, slit width 10 cm^{-1}, time constant 15 s, scanning speed 0.1 cm^{-1}/s.

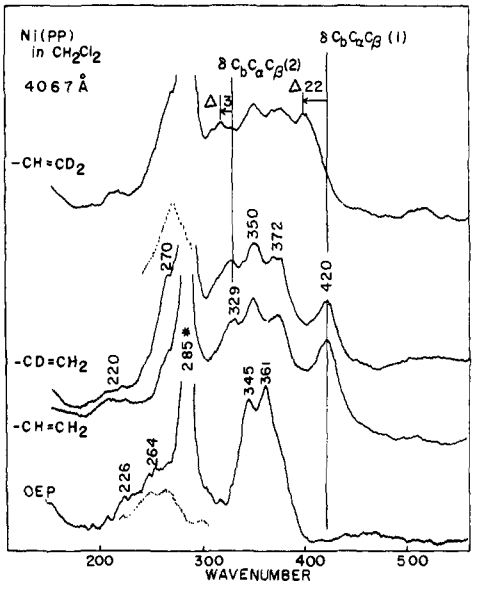

Figure 5. Low-frequency RR spectra of NiOEP, NiPP, NiPP-d_α and NiPP-$d_{2\beta}$, in CH_2Cl_2 (responsible for the 285-cm^{-1} band), excited at 4067 Å excitation. The bands inserted with broken lines are from spectra in benzene solutions. Conditions: laser power 100 mW, slit width 8 cm^{-1}, time constant 15 s, scanning speed 0.1 cm^{-1}/s.

the two nearly degenerate highest filled π orbitals (a_{1u}, a_{2u}) and the degenerate lowest unfilled π^* orbitals (e_g).[19] Resonance with the intense B band, near 400 nm, enhances Raman bands associated with totally symmetric vibrations, A_{1g}, while excitation in the Q_0 and Q_1 bands at ~550 and ~500 nm produces selective enhancement of non totally symmetric modes, A_{2g}, B_{1g}, and B_{2g}, which are effective in mixing the Q and B transitions.[20] All of these are in-plane modes. (The symmetric stretch of a pair of equivalent axial ligands is also A_{1g}, but Ni porphyrins have no axial ligands.) The remaining in-plane modes, E_u, are infrared active. Raman enhancement is expected for porphyrin skeletal vibrations, including those involving the C_b-substituent bonds, but not for internal modes of saturated substituents. Kitagawa et al.[10] were able to assign all the observed Raman bands of NiOEP by treating the ethyl groups as point masses. In this model there are 53 in-plane modes, classified as

$$\Gamma_{\text{in-plane}} = 9A_{1g} + 8A_{2g} + 9B_{1g} + 9B_{2g} + 18E_u$$

In this work we have adopted the NiOEP assignments and numbering scheme of Kitagawa et al. (Table II). We have located a depolarized RR band, at 1482 cm^{-1} in both NiOEP and NiPP, with 5682-Å excitation, which we assign to ν_{28} (B_{2g}), calculated by Abe et al.[11] at 1469 cm^{-1}. Kitagawa et al.[10] observed a weak 1483-cm^{-1} band with 5145-Å excitation, which they recorded as anomalously polarized and were unable to assign. The vinyl groups of NiPP do not alter the basic mode symmetries or RR enhancement patterns, and it is in most cases straightforward to correlate the NiPP skeletal modes with those of NiOEP. Table I shows that the RR depolarization ratios are in essentially quantitative accord, except for the A_{2g} modes, which are particularly sensitive to symmetry-lowering effects.[20]

The NiPP vinyl groups are, however, conjugated with the aromatic system, and they can be expected to perturb the NiOEP spectrum. Two kinds of influences have been anticipated[12] and are in fact observed: (1) By virtue of their asymmetric disposition (Figure 1), the vinyl groups destroy the porphyrin symmetry center and can consequently induce Raman activity in IR modes, and

(19) Gouterman, M. In "The Porphyrins"; Dolphin, D., Ed.; Academic Press: New York, 1978; Vol. IV, pp 1-156.

(20) Spiro, T. G.; Strekas, T. C. (1972) *Proc. Natl. Acad. Sci., U.S.A.* **1972**, *69*, 2622.

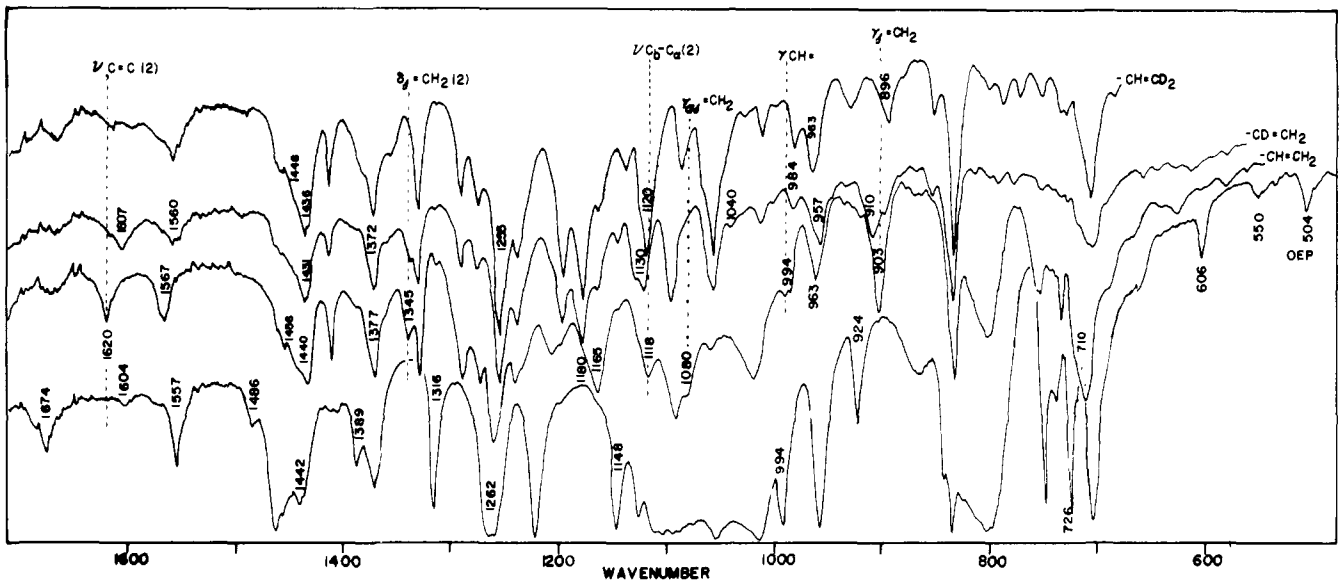

Figure 6. FTIR spectra of NiOEP, NiPP, NiPP-d_a, and NiPP-$d_{2\beta}$ in CsI pellets. Conditions: resolution 1 cm^{-1}, sensitivity 4.

Table I. Observed Raman Bands (cm^{-1}) and Depolarization Ratio (ρ)

		NiOEP							
			λ_{exc}, Å				λ_{exc}, Å		
		ν	4067	5145	5682	ν	4131	5145	5682
ν_{10}[a]	B_{1g}[a]	1655	0.75	0.75	0.75	1655	0.75	0.75	0.75
						1634	0.40		
ν_{37}	E_u	(1604)[b]				1610	0.30		
ν_{19}	A_{2g}	1603		6.0	1.4	1603		3.0	2.3
ν_2	A_{1g}	1602	0.23			1593	0.25		
ν_{11}	B_{1g}	1576	0.75	0.75	0.75	1575			0.87
ν_{38}	E_u	(1557)[b]				1566	0.3	w	
ν_3	A_{1g}	1519	0.2	0.2		1519	0.3	0.3	
ν_{28}	B_{2g}	1482			0.7	1482			0.8
						1434	0.71	0.75	dp
ν_{29}	B_{2g}	1409	0.75	0.75	0.75	1401	dp	0.78	dp
ν_{20}	A_{2g}	1396		∞	ap	1399		ap	ap
ν_4	A_{1g}	1383	0.12	0.12	P	1381	0.17	0.17	p
						1343		1.23	1.3
ν_{21}	A_{2g}	1305		11.5	2.8	1305		4.47	∞
						1305	P		
$\nu_5 + \nu_9$	A_{1g}	1261	0.3			1254	w(sh)	w(sh)	
ν_{13}	B_{1g}	1220	0.7	0.7	0.7	1234	0.75	0.8	0.7
ν_{30}	B_{2g}	1159	0.75	0.8	dp	1167	0.7	0.7	dp
$\nu_6 + \nu_8$	A_{1g}	1138	0.2		P	1130	0.25		
ν_{22}	A_{2g}	1121		∞	0.9	1125		ap	0.7
						1089			0.2
ν_5	A_{1g}	1025	0.3	0.3	0.5				
ν_{45}	E_u					999			0.3
						999			0.3
$\nu_{32} + \nu_{35}$	A_{1g}	963			P	969	P		0.5
ν_6	A_{1g}	806	P		0.14	805			P
ν_{32}	B_{2g}	782			0.75	782			dp
$\nu_{33} + \nu_{34}$	A_{1g}	770			P	771			P
ν_{16}	B_{1g}	752	0.71	dp	0.7	752	0.7		0.6
ν_7	A_{1g}	674	0.13	P	0.1	675	0.12		0.1
						420	P		P
$2\nu_{35}$	A_{1g}	361	0.13		P	372	0.1		w
ν_8	A_{1g}	345	0.17		P	350	0.2		P
						330	P		
ν_{52}	E_u	264	P			270	P		P
ν_9	A_{1g}	226	P			220	P		P

[a] Mode numbering and assignments follow Kitagawa et al.;[10] this is the first observation of ν_{28} (B_{2g}). [b] Bands in the NiOEP IR spectrum corresponding to observed NiPP RR (and IR) bands.

vice versa. The degeneracy of the E_u modes can also be lifted. (2) The characteristic local modes of the vinyl groups, possibly perturbed by interactions with the skeletal modes, can contribute directly to the IR and Raman spectra; RR intensity depends on the extent of vinyl mode involvement in the excited-state distortion and on vibrational coupling with active skeletal modes. The remaining NiPP substituents, methyl and propionic ester, are electronically and vibrationally similar to ethyl groups, although the coupling of C–H deformation modes may differ somewhat.

B. Vinyl Modes. The CH=CH$_2$ group has 10 internal vibrational modes. Three of these are C–H stretches in the ~3000-cm^{-1} region, which are not expected to show RR enhance-

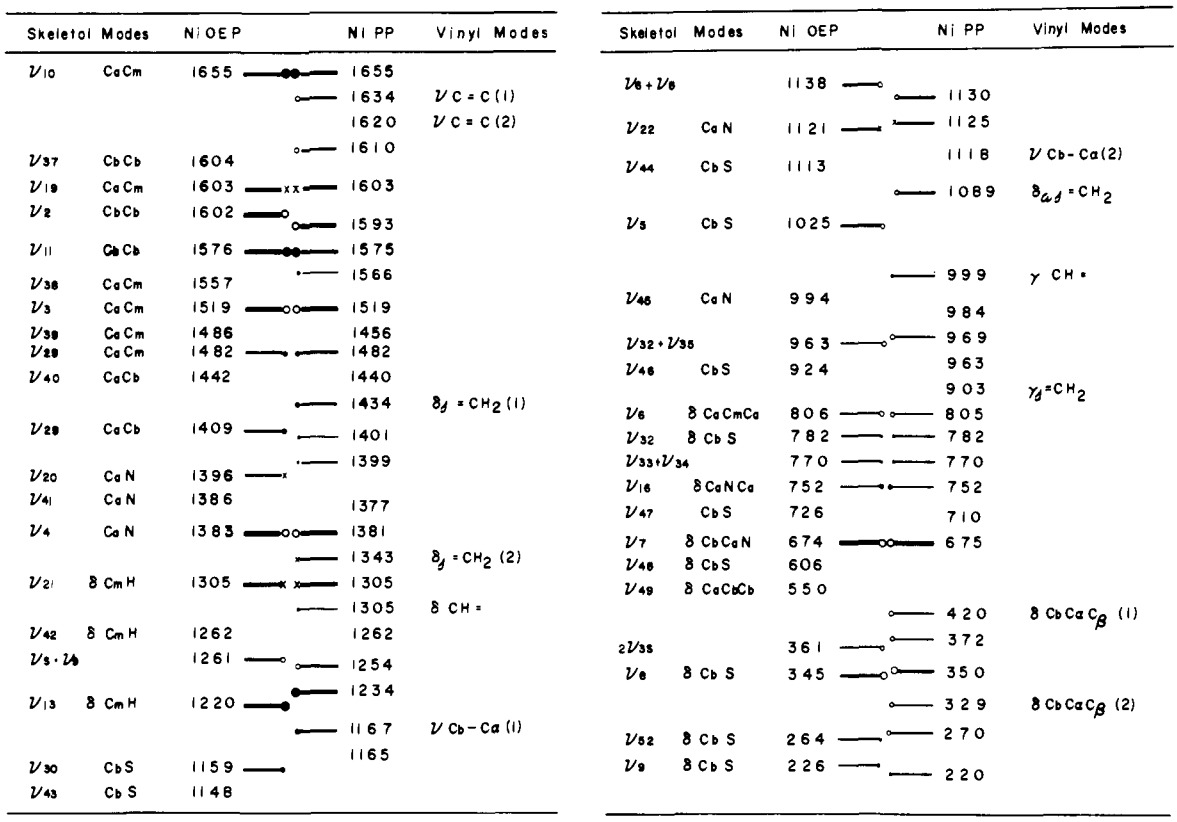

Figure 7. Schematic diagram of the RR (solid lines) and IR (dashed lines) modes of NiOEP and NiPP, with assignments of the skeletal (left) and vinyl (right) modes. The major contributor to each skeletal mode is indicated next to the mode number. The symbols indicate the RR polarizations: O, polarized; ●, depolarized: ×, anomalously polarized. The sizes of the symbols indicate the selective intensities of the RR bands at the wavelengths of greatest enhancement.

ment and have not been included in this study. The remaining seven are diagrammed in Figure 8, with typical values of their frequencies.[21] They consist of the double bond stretch, ν(C=C); three in-plane deformations, δ(=CH_2) (CH_2 symmetric deformation), δ(CH=) (CH deformation), δ_{as}(=CH_2) (CH_2 asymmetric deformation); and three out-of-plane deformations, γ(CH=) (CH wag), γ_s(=CH_2) (CH_2 symmetric wag), γ_{as}(=CH_2) (CH_2 asymmetirc wag).

The vinyl modes are identifiable via their deuteration shifts and by comparison with simple olefins, particularly styrene, for which complete assignments and CD=CD_2 deuteration shifts have been given by Condirston and Liposa.[22] Since there are two vinyl substituents in NiPP, however, these vinyl modes occur in pairs, consisting of the in-phase and out-of-phase combinations of the local modes. To a first approximation, these pairs are expected to be coincident, because the vinyl groups are spatially well separated. They may, however, be split by different interactions with nearby porphyrin modes. Several such splittings are in fact observed, either as a difference between Raman and IR frequencies for a given vinyl mode or a doubling of the Raman bands. The coupling with skeletal modes probably accounts for most of the RR intensity of the vinyl modes. It would otherwise be surprising that most of these modes can be detected at all in the RR spectra. The variable excitation pattern (some vinyl modes are seen in B-band, excitation, others in Q-band excitation) is also consistent with an intensity mechanism involving selective coupling with skeletal modes.

In addition to these internal modes, there is a ring–vinyl stretch, $\nu(C_b-C_\alpha)$, and two deformation modes involving the vinyl group as a whole: one is centered at the vinyl C_α atom, $\delta(C_bC_\alpha C_\beta)$, and the other is centered at the pyrrole C_b atom, $\delta(C_bC_bC_\alpha)$. Neither $\nu(C_b-C_\alpha)$ nor $\delta(C_bC_bC_\alpha)$ adds to the vibrational count given above for NiOEP; they are included in the sets of vibrations involving the point mass substituents, i.e., $\nu(C_b-S)$. The vinyl and ethyl frequencies may, however, differ appreciably.

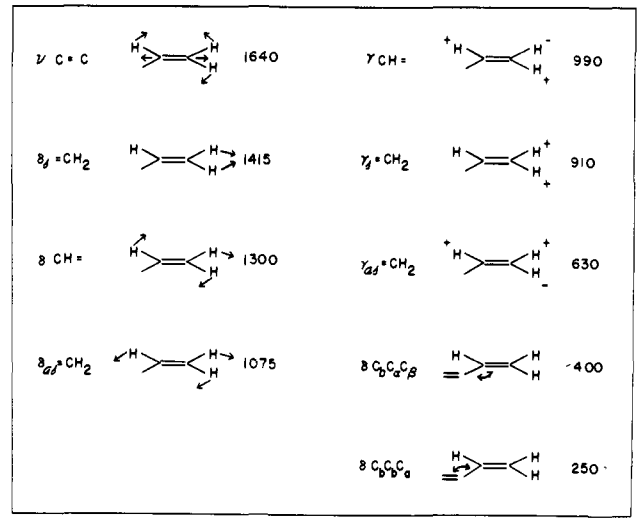

Figure 8. Schematic diagram of the vinyl modes.

Table III lists our vinyl assignments for NiPP and its deuterated forms along with those of styrene. Where two Raman bands are assigned to the same vinyl local mode, they are labeled (1) and (2) in order of decreasing frequency. Discussion of these assignments follows:

ν(C=C). The double bond stretch is expected at ~1630 cm^{-1} and is moderately sensitive to C_α and C_β deuteration, e.g., 1640, 1625, and 1603 cm^{-1} for 1-hexene, 1-hexene-d_α, and 1-hexene-$d_{2\beta}$, respectively.[23] NiPP, but not NiOEP, shows an IR band at 1620

(21) Colthup, N. B.; Daly, L. H.; Wiberly, S. E. "Introduction to IR and Raman Spectroscopy"; Academic Press: New York, 1975; pp 246–252.
(22) Condirston, D. A.; Liposa, J. D. *J. Mol. Spectrosc.* **1976**, *63*, 466.
(23) Hoffmann, E. G. *Liebigs Ann. Chem.* **1958**, *618*, 276.

Table II. Summary of Raman and IR Bands (cm^{-1}) Assignable to Skeletal or Vinyl Modes

		NiOEP		NiPP		NiPP-d_α		NiPP-$d_{2\beta}$		
no.		R	IR	R	IR	R	IR	R	IR	vinyl assignment
ν_{10}[a]	B_{1g}[a]	1655		1655		1655		1655		
				1634		~1610		~1600		ν(C=C (1))
					1620		1607		?	ν(C=C (2))
ν_{37}	E_u		1604	1610	?	~1610	?	~1610	?	
ν_{19}	A_{2g}	1603		1603		1603		1603		
ν_2	A_{1g}	1602		1593		1590		~1590		
ν_{11}	B_{1g}	1576		1575		1575		1575		
ν_{38}	E_u		1557	1566	1567	~1560	1560	~1560	1560	
ν_3	A_{1g}	1519		1519		1519		1519		
ν_{39}	E_u		1486		1456		1448		1448	
ν_{28}	B_{2g}	1482		1482		1482		1482		
ν_{40}	E_u		1442		1440		1431		1436	
				1434		1425				δ_s(=CH_2 (1))
ν_{29}	B_{2g}	1409		1401		~1402		1409		
ν_{20}	A_{2g}	1396		1399		~1399		1395		
ν_{41}	E_u		1386		1377		1372		1372	
ν_4	A_{1g}	1383		1381		1381		1381		
				1343	1345	1338	1340			δ_s(=CH_2 (2))
ν_{21}	A_{2g}	1305		1305		1305		1305		
				1305		1096		1305		δ(CH=)
ν_{42}	E_u		1262		1262		1255		1255	
$\nu_5 + \nu_9$	A_{1g}	1261		1254		1254		1254		
ν_{13}	B_{1g}	1220		1234		1234		1234		
ν_{30}	B_{2g}	1159		1167		1152		1167		
ν_{43}	E_u		1148	1167	1165	1180	1180	1167		$\nu(C_b-C_\alpha)$ (1)
$\nu_6 + \nu_8$	A_{1g}	1138		1130		1130		1130		
ν_{22}	A_{2g}	1121		1125		1125		1125		
ν_{44}	E_u		1113		1118		1130		1120	$\nu(C_b-C_\alpha)$ (2)
				1089	1080	1039	1040		896	δ_{as}(=CH_2)
ν_5	A_{1g}	1025								
				999	994				932	γ(CH=)
ν_{45}	E_u		994	999	984	999	984	999	984	
$\nu_{32} + \nu_{35}$	A_{1g}	963		969		969		969		
ν_{46}	E_u		924		963		957		963	
					903		910			γ_s(=CH_2)
ν_6	A_{1g}	806		805		805		805		
ν_{32}	B_{2g}	782		782		782		782		
$\nu_{33} + \nu_{34}$	A_{1g}	770		770		770		770		
ν_{16}	B_{1g}	752		752		752		752		
ν_{47}	E_u		726		710		710		710	
ν_7	A_{1g}	674		675		675		675		
ν_{48}	E_u		606		?		?		?	
ν_{49}	E_u		550		?		?		?	
				420		420		408		$\delta(C_bC_\alpha C_\beta$ (1))
$2\nu_{35}$	A_{1g}	361		372		372		372		
ν_8	A_{1g}	345		350		350		350		
				329		329		316		$\delta(C_bC_\alpha C_\beta$ (2))
ν_{52}	E_u	264	(287)[b]	270		270		270		
ν_9	A_{1g}	226		220		220		220		

[a] Skeletal assignments follow Kitagawa et al.[10] [b] Observed in the IR spectrum of Ogoshi.[26]

cm^{-1}, which shifts to 1607 cm^{-1} for NiPP-d_α and is obscured for NiPP-$d_{2\beta}$. With 4131-Å excitation a deuterium-sensitive RR band is seen at 1634 cm^{-1}; its d_α and $d_{2\beta}$ shifts are uncertain since the band moves under other bands at 1610 and 1593 cm^{-1}, respectively. The 14-cm^{-1} IR–Raman difference for ν(C=C) is attributed to splitting of the in- and out-of-phase combinations, as described above. Earlier an "extra" band at 1620 cm^{-1} in hemoglobin RR spectra had been suggested to be the vinyl C=C stretch.[12] This is confirmed by FePP deuteration shifts.[17]

δ_s(=CH_2). The vinyl CH_2 scissors mode is usually seen at ~1415 cm^{-1}, but the NiPP RR spectra show two flanking bands, at 1434 and 1343 cm^{-1}, which shift 9 and 5 cm^{-1} for NiPP-d_α and disappear for NiPP-$d_{2\beta}$. These must both be assigned to δ_s(=CH_2), the large splitting implying strong and differential interactions with skeletal modes. In the IR spectrum, the 1434-cm^{-1} region is obscured by numerous CH deformation modes, but a 1345-cm^{-1} NiPP IR band is seen to shift to ~1342 cm^{-1} for d_α and disappear for $d_{2\beta}$.

The 1434-cm^{-1} RR band is depolarized (dp) and interacts with the dp mode at 1401 cm^{-1} (ν_{29}, B_{2g}); this is evident from the increase of the 1401-cm^{-1} band to 1409 cm^{-1}, the same frequency as in NiOEP, when the coupling is relieved by C_β deuteration (Figure 3). The 1343-cm^{-1} mode, which is sometimes quite strong in protoheme proteins,[12,13] is anomalously polarized (ap) and is probably coupled with the ap mode at ~1399 cm^{-1} (ν_{20}, A_{2g}—its exact position is uncertain because of overlap with the 1401 dp mode), which is ~4 cm^{-1} higher than for NiOEP. The 5682-Å spectrum (Figure 4) suggests a downward shift of the 1394-cm^{-1} band for NiPP-$d_{2\beta}$, as expected, although the band is weak and poorly defined. It is of interest that Abe et al.'s[11] calculated eigenvectors for ν_{29} and ν_{20}, although mainly C–N stretching in character, show substantial involvement of the C_b-substituent bonds. Due to the different symmetries, the stretching of these bonds shows the same phase for adjacent pyrrole rings in the case of ν_{20} but opposite phase in the case of ν_{29}. Thus the mode symmetries provide a natural explanation for differential coupling to the in- and out-of-phase combinations of the vinyl CH_2 scissors vibrations.

δ(CH=). The 4131-Å RR spectrum (Figure 2) shows a weak band at 1305 cm^{-1}, the same frequency as δ(CH=) of styrene. It disappears for NiPP-d_α, and a new band appears at 1096 cm^{-1}, which is suggested to be δ(CD=), its intensification due to mixing

Table III. Vinyl Frequencies (cm^{-1})

description	styrene/ styrene-d_3[a]	NiPP/NiPP-d_α/NiPP-$d_{2\beta}$ RR	IR
ν(C=C (1))[b]	1630/1562	1634/~1610/~1600	
ν(C=C (2))			1620/1607/-
δ_s(=CH_2) (1)	1411/1048	1434/1425/-	
δ_s(=CH_2) (2)		1343/1338/-	1345/1342/-
δ(CH=)	1305/1003	1305/1096/1305	
ν(C_b–C_α) (1)	1203/1223	1167/1182/1167	
ν(C_b–C_α) (2)			1118/1130/1120
δ_{as}(=CH_2)	1032/831	1089/1038/-	1080/1040/896
γ(CH=)	992/788	999/-/-	994/-/932
γ_s(=CH_2)	909/709		903/910/-
γ_{as}(=CH_2)	640/571		
δ($C_bC_\alpha C_\beta$) (1)	554/510 or	420/420/398	
δ($C_bC_\alpha C_\beta$) (2)	442/420	330/330/316	

[a] From ref 22. [b] (1) and (2) identify separate modes corresponding to the same local motion but alternate phasing of the two protoporphyrin IX vinyl groups.

with the nearby 1130-cm^{-1} (A_{1g}) and 1125-cm^{-1} (A_{2g}) modes. No IR band is seen for δ(CH=); its IR intensity is usually low.[21]

$\nu(C_b–C_\alpha)$. In styrene[22] the vinyl–ring stretch, at 1203 cm^{-1}, is characterized by a 20-cm^{-1} upshift upon deuteration, due to the uncoupling of the δ(CH=) mode at 1305 cm^{-1}. A 15-cm^{-1} upshift is seen for the 1167-cm^{-1} RR band of NiPP (Figure 3) and also for a coincident IR band (Figure 6), while a 12-cm^{-1} upshift is seen for the 1118-cm^{-1} IR band, upon C_α deuteration. These are therefore assigned to the two ring–vinyl modes; they belong to the set of eight ring-substituent stretches and correlate with the 1148-cm^{-1} (ν_{43}, E_u) and 1113-cm^{-1} (ν_{44}, E_u) modes of NiOEP. The higher, but not the lower, E_u mode is evidently activated in the NiPP RR spectrum.

An extra band is found (Figure 3) in the NiPP-d_α RR spectrum at 1152 cm^{-1}, making it appear that the 1167-cm^{-1} NiPP band is split into two components. We tentatively identify this band with the 1159-cm^{-1} B_{2g} mode (ν_{30}) of NiOEP, which seems to move up to 1167 cm^{-1} for NiPP (and NiPP-$d_{2\beta}$) and back down to 1152 cm^{-1} for NiPP-d_α.

δ_{as}(=CH_2). The vinyl CH_2 rock is expected[21] at ~1075 cm^{-1} and is assigned to the 1089-cm^{-1} RR band (Figure 4), shifting to 1038 cm^{-1} for d_α and disappearing for $d_{2\beta}$. Curiously this band, although polarized, appears with Q_0-band but not with B-band (Figure 2) excitation; its intensification may result from specific interactions with the polarized band at 999 cm^{-1}, which appears to be an activated E_u mode (ν_{45}). In the IR spectra, δ_{as}(=CH_2) can be assigned to bands at 1080, 1040, and 896 cm^{-1} for NiPP, NiPP-d_α, and NiPP-$d_{2\beta}$.

γ(CH=). The out-of-plane CH= wag is expected at ~990 cm^{-1} and can be assigned to the NiPP IR band at 994 cm^{-1}, which disappears in d_α and appears to shift to 932 cm^{-1} in $d_{2\beta}$. The substantial $d_{2\beta}$ shifts is expected since coupling with γ_{as}(=CH_2) is strong; the two modes can alternatively be described as "trans" and "cis" CH wags[21] (see Figure 8). RR enhancement is not expected, but in fact significant intensity is lost from the coincident 999-cm^{-1} RR band, assigned to skeletal mode ν_{45} (E_u), upon C_α or C_β deuteration (Figure 4). For the complex $Im_2Fe^{II}PP$ (Im = imidazole), a high-energy shoulder on its 997-cm^{-1} RR band is definitely lost on vinyl deuteration.[17] The enhancement is no doubt due to the accidental degeneracy of γ(CH=) with ν_{45}.

γ_s(=CH_2). The symmetric =CH_2 wag is expected at ~910 cm^{-1} and does not mix with =CH wagging. It is assigned to the 903-cm^{-1} NiPP IR band, which is at 910 cm^{-1} for d_α and disappears for $d_{2\beta}$. It does not appear in the RR spectra.

γ_{as}(=CH_2). The asymmetric =CH_2 wag, expected around 630 cm^{-1}, is usually not seen in the IR spectrum and was observed for styrene as a weak Raman mode.[22] We have been unable to locate it for NiPP.

$\delta(C_bC_\alpha C_\beta)$. In styrene, the C_α bend was suggested[22] to be at either 554 or 442 cm^{-1}. In the 4067-Å NiPP RR spectrum (Figure 5), we observe bands at 420 and 330 cm^{-1}, not present in the spectrum of NiOEP, which shift down for $d_{2\beta}$ but not for d_α. This behavior is expected for C_α bending, since the C_α–H bond bisects the C_b—C_α=C_β angle, and the H (or D) atom moves very little during the vibration. The large separation of the two modes implies substantial coupling with porphyrin skeletal modes.

$\delta(C_bC_bC_\alpha)$. This coordinate should contribute to modes at even lower frequency. Abe et al.[11] calculate significant $\delta(C_bC_bS)$ contributions for several modes in the 200–400-cm^{-1} region. We located no additional d_α or $d_{2\beta}$ shifts in either the RR or IR spectra that would locate a specific $\delta(C_bC_bC_\alpha)$ contribution.

C. E_u-Type Raman Modes. Vinyl induction of Raman activity into IR modes can be clearly seen in the extra NiPP RR bands at 1610 and 1566 cm^{-1} with 4131-Å excitation (Figure 2). These correlate with the two highest NiOEP E_u modes, ν_{37} and ν_{38}, at 1604 and 1557 cm^{-1}. The 1604-cm^{-1} IR band is very weak and is not observed for NiPP. The 1557-cm^{-1} IR band is stronger and shifts to 1567 cm^{-1} for NiPP, in coincidence with the RR band. It shifts back to 1560 for NiPP-d_α and -$d_{2\beta}$, indicating significant interaction with the vinyl modes. (These shifts cannot be seen in the RR spectra because of overlapping bands.)

The 1167-cm^{-1} RR band of NiPP correlates with both the 1159-cm^{-1} B_{1g} and 1148-cm^{-1} E_u modes of NiOEP; ring–vinyl stretching is directly involved in this case (see above). The 999-cm^{-1} RR band (p) correlates with the 993-cm^{-1} Eu mode (ν_{45}), as does an IR band at 984 cm^{-1}. All of them shift appreciably upon meso -d_4 substitution. (The d_4 shifts 999 cm^{-1} → 972 cm^{-1} in the RR spectrum of $Im_2Fe^{II}PP$ and 984 cm^{-1} → 968 cm^{-1} in the IR spectrum of $(Cl)Fe^{III}PP$ have been observed: S. Choi unpublished results.) The RR–IR separation (15 cm^{-1}) may reflect a splitting of the E_u components. There is a NiPP RR band at 270 cm^{-1} that is much weaker in the NiOEP spectrum; it is tentatively assigned to ν_{52} (E_u), calculated by Abe et al. at 264 cm^{-1}. None of the other E_u modes are seen in the RR spectra. Some of them would be obscured by stronger RR bands, but others, e.g., ν_{39}, at 1456 cm^{-1}, occur in blank regions of the RR spectra and are definitely not activated significantly.

Interestingly, there is no observable IR activation of Raman modes. For example, the strong NiPP Raman modes at 1655, 1603, 1593, and 1519 cm^{-1} all occur in clear regions of the IR spectrum and show no trace of activity. This observation suggests that vinyl conjugation occurs mainly in the excited state since IR intensity depends on the ground-state electron distribution while RR enhancement depends on the change in electronic structure between ground and excited states. There is, however, some evidence for ground-state conjugation in the skeletal mode frequency pattern observed for Fe complexes.[17]

D. Vinyl Influences on Skeletal Frequencies. Deuteration of the vinyl groups shifts the frequencies of those skeletal modes with which the vinyl modes are strongly coupled. The 1401-cm^{-1} (ν_{29}, B_{2g}) and 1395-cm^{-1} (ν_{20}, A_{2g}) modes, which are believed to couple with the δ_s(=CH_2) modes and the 1167-cm^{-1} (ν_{30}, B_{2g}) mode coupled to $\nu(C_b–C_\alpha)$, have already been discussed. C_α or C_β deuteration also produce a 3-cm^{-1} downshift in the polarized Raman band at 1593 cm^{-1} (ν_2, A_{1g}) and 7–8-cm^{-1} downshifts in the IR bands at 1567 and 1456 cm^{-1} (ν_{38} and ν_{39}, E_u), which are probably coupled to the ν(C=C) modes at 1634 (Raman) and 1620 (IR) cm^{-1}. There is a curious intensification in the region of the 1603-cm^{-1} (ν_{19}, A_{2g}) RR band on C_α or C_β deuteration, in the 5682-Å but not the 5145-Å spectrum (Figures 3 and 4). Apparently either ν(C=C) (1) or ν(C=C) (2), both of which shift into this region on deuteration, gain intensity with Q_0 but not with Q_1 excitation, via coupling with the nearly coincident A_{2g} skeletal mode. NiPP also shows a number of skeletal frequency shifts relative to NiOEP, as illustrated in Figure 7; in part these reflect the vinyl mode couplings, although the other peripherial substitutions (methyl and propionic acid for ethyl) may also play a role, which remains to be elucidated in further studies. Thus $\nu_2(A_{1g})$ at 1593 cm^{-1} is 10 cm^{-1} lower than in NiOEP, in the direction expected for coupling with ν(C=C), but the flanking E_u modes, ν_{37} and ν_{38}, are 6 and 9 cm^{-1} higher than in NiOEP. ν_{29} (B_{2g}) at 1401 cm^{-1} is lower by 8 cm^{-1}, while ν_{20} (A_{2g}) at 1399 cm^{-1} is higher by 4 cm^{-1}, due to coupling with δ_s(=CH_2) (1) and (2),

as already noted. Several differences are seen between 1300 and 900 cm^{-1}, as expected from the major contributions of C_b-substituent stretching to the modes in this region:[11] 1261 → 1254 ($\nu_5 + \nu_9$, A_{1g}), 1220 → 1234 (ν_{13}, B_{1g}), 1159 → 1167 (ν_{30}, B_{2g}), 1148 → 1167 (ν_{43}, Eu), 1138 → 1130 ($\nu_6 + \nu_8$, A_{1g}), 1113 → 1118 (ν_{44}, E_u), and 963 → 969 ($\nu_{32} + \nu_{35}$, A_{1g}) cm^{-1}, between NiOEP and NiPP. Curiously, the 1025-cm^{-1} band (p) of NiOEP, assigned by Kitagawa et al.[10] to ν_5 (A_{1g}) and calculated[11] to be mainly C_b-substituent stretching in character, is absent in the NiPP spectrum. It reappears in mesoporphyrin (MP) complexes (see following article[17]); MP differs from PP only in the replacement of vinyl with ethyl groups. Thus the loss in 1025-cm^{-1} intensity is a specific vinyl effect. Finally, appreciable differences are seen for the low-frequency skeletal modes, containing C_b-substituent bending contributions,[11] which are flanked by the two $\delta(C_bC_\alpha C_\beta)$ modes: 361 → 372 ($2\nu_{35}$, A_{1g}) and 345 → 350 (ν_8, A_{1g}) cm^{-1}.

Many frequencies are not shifted at all between NiOEP and NiPP, however. These include the most prominent Raman modes, at 1655 (ν_{10}, B_{1g}), 1603 (ν_{19}, A_{2g}), 1576 (ν_{11}, B_{1g}), 1519 (ν_3, A_{1g}), and 1383 (ν_4, A_{1g}) cm^{-1}, which have previously been identified as structure-marker bands I–V[24] in Fe porphyrins and heme proteins. Their lack of substituent sensitivity, which was exploited in the use of mesoporphyrin analogues in order to obtain less cluttered RR spectrum,[24] is consistent with the absence of significant perturbation by the peripheral substituents on the ground-state skeletal structure. For metalloporphyrins with the same metal ions and ligands, alteration of the peripheral substituents is found to be without appreciable influence on the skeletal bond lengths and angles.[25]

Conclusions

Comparison of IR and variable excitation RR spectra of NiOEP and NiPP and examination of the effects of selective vinyl deuteration have provided identification of the vinyl modes and their influences on the skeletal modes. The following points emerge from this analysis:

(1) The vinyl modes couple significantly to porphyrin skeletal modes, as shown by several splittings of the in- and out-of-phase combinations; in two cases ($\delta_s(=CH_2)$ and $\delta(C_bC_\alpha C_\beta)$) the splittings are close to 100 cm^{-1}. Such coupling is probably responsible for the observed enhancement of most of the vinyl modes in the RR spectra.

(2) In turn these couplings affect the skeletal modes, several of which are shifted from the frequencies characteristic of NiOEP. Several skeletal modes are not affected, however, including some previously identified as structure markers for heme proteins.

(3) The vinyl groups do not alter the basic skeletal mode symmetries (RR depolarization ratios do not change significantly) or enhancement patterns. They do, however, induce appreciable Raman intensity into some of the E_u modes, reflecting loss of the symmetry center via the asymmetric conjugation. The absence of Raman modes in the IR spectrum suggests, however, that vinyl conjugation occurs mainly in the excited state.

The availability of the NiPP vibrational assignments can be expected to lead to more definite and reliable interpretation of heme protein RR spectra than has heretofore been possible. This theme is taken up in the following paper.

Experimental Section

The preparation of protoporphyrin IX deuterated at the C_α or C_β vinyl positions is described elsewhere.[27] Standard procedures were used for nickel(II) insertion.[28] Solutions for Raman spectroscopy were prepared to an absorbance of ~1.0/mm in CCl_4 for the region >900 cm^{-1} or in CH_2Cl_2 for the region <900 cm^{-1}. Spectra were excited with CW Kr^+ (4131 and 5638 Å) or Ar^+ (5145 Å) lasers, incident on the sample in a spinning cell, and were recorded with a Spex 1401 double monochromator with a photomultiplier and photon-counting electronics. IR spectra were obtained on solid samples in CsI pellets with a Digilab FTIR spectrometer.

Acknowledgment. This work was supported by NIH Grants HL 12526 (to T.G.S.) and HL 22252 (to K.M.S.). We thank Dr. Paul Stein for many helpful discussions about the spectral assignments.

Registry No. NiOEP, 24803-99-4; NiPP, 15304-70-8.

(24) Spiro, T. G.; Burke, J. M. *J. Am. Chem. Soc.* **1976**, *98*, 5482.
(25) Hoard, J. L. In "Porphyrins and Metalloporphyrins"; Smith, K. M., Ed.; American Elsevier: New York, **1976**, pp 317–376.
(26) Ogoshi, H.; Masai, N.; Yoshida, Z.; Takemoto, J.; Nakamoto, K. *Bull. Chem. Soc. Jpn*, **1971**, *44*, 49.
(27) Budd, D. L.; LaMar, G. N.; Langry, K. C.; Smith, K. M.; Nayyir-Mazhir, R. *J. Am. Chem. Soc.* **1979**, *101*, 6091.
(28) Buchler, J. W. In "Porphyrins and Metalloporphyrins"; Smith, K. M., Ed.; American Elsevier: New York, **1976**, pp 157–231.